



# A Study on Three Factors Influencing Uptake Rates of Nitric Acid onto Dust Particles

Chul Han Song\* and Chung Man Kim<sup>1)</sup>

Department of Environmental Science and Engineering, Gwangju Institute of Science and Technology (GIST),  
1 Oryong-dong, Buk-gu, Gwangju 500-712, Korea

<sup>1)</sup>Korea Ocean Research & Development Institute (KORDI), 104 Sinseong-ro, Yuseong-gu, Daejeon 305-343, Korea

\*Corresponding author. Tel: +82-62-715-3276, E-mail: chsong@gist.ac.kr

## ABSTRACT

Recent studies have indicated that the observed nitric acid ( $\text{HNO}_3$ ) uptake rates ( $R_{\text{HNO}_3}$ ) onto dust particles are much slower than  $R_{\text{HNO}_3}$  used in the previous modeling studies. Three factors that possibly affect  $R_{\text{HNO}_3}$  onto dust particles are discussed in this study: (1) the magnitude of reaction probability of  $\text{HNO}_3$  ( $\gamma_{\text{HNO}_3}$ ), (2) aerosol surface areas, and (3) gas-phase  $\text{HNO}_3$  mixing ratio. Through the discussion presented here, it is shown that the use of accurate  $\gamma_{\text{HNO}_3}$  is of primary importance. We suggest that the use of  $\gamma_{\text{HNO}_3}$  values between  $\sim 10^{-3}$  and  $\sim 10^{-5}$  produces more realistic results than the use of  $\gamma_{\text{HNO}_3}$  values between  $\sim 10^{-1}$  and  $\sim 10^{-2}$  does, more accurately modeling the nitrate formation characteristics on/in dust particles. We also discuss two different types of aerosol surface area, active and geometric, since the use of different aerosol surface areas often leads to an erroneous result in  $R_{\text{HNO}_3}$ . In addition, the levels of the gas-phase  $\text{HNO}_3$  are investigated with the example cases of TRACE-P DC-8 flights in East Asia. The  $\text{HNO}_3$  levels were found to be relatively high, indicating that they can not limit nitrate formation in dust particles.

**Key words:** Reaction probability, Dust particles, Nitric acid, Uptake rates, Aerosol surface area

## 1. INTRODUCTION

Recently, several studies have reported that although East Asian dust particles have sufficient chemical aging (or contacting) times (say, 1-4 days) with atmospheric air pollutants, they were found to contain only small amounts of nitrate (and/or sulfate) (Song *et al.*, 2007; Song *et al.*, 2005; Maxwell-Meier *et al.*, 2004). This fact possibly indicates that the gas-to-particle nitric acid ( $\text{HNO}_3$ ) uptake rates ( $R_{\text{HNO}_3}$ ) onto dust particles are slower than previously estimated. This could also be an important correction to the results from pre-

vious studies (Meskhidze *et al.*, 2003; Song and Carmichael, 2001; Zhang and Carmichael, 1999; Dentener *et al.*, 1996). For example, Meskhidze *et al.* (2003) inferred from the data of TRACE-P DC-8 Flight #13 that total nitrate ( $=\text{HNO}_3(\text{g})+\text{NO}_3^-(\text{p})$ ) distribution between gas phase and East Asian dust particles reaches a near equilibrium (refer to Fig. 4 in Meskhidze *et al.* (2003)). Their work supported the opposite idea that dust particles could contain a quite large amount of nitrate that could completely neutralize dust-originated cationic components such as  $\text{Ca}^{2+}$  and  $\text{Mg}^{2+}$ . This study, therefore, intends to discuss possible causes of this discrepancy in order to offer a convincing explanation.

Closely connected with this issue, controversy has continued regarding the magnitude of reaction probability of  $\text{HNO}_3$  ( $\gamma_{\text{HNO}_3}$ ) onto dust particles. Several research groups measured  $\gamma_{\text{HNO}_3}$  onto various types of dust particle, from proxy species of dust particles (e.g.,  $\alpha\text{-Al}_2\text{O}_3$ ,  $\text{SiO}_2$ ,  $\text{CaCO}_3$  etc) to authentic Saharan and Gobi dust. However, a large difference in the magnitude of  $\gamma_{\text{HNO}_3}$  onto dust particles has been reported (Johnson *et al.*, 2005; Umann *et al.*, 2005; Harnisch and Crowley, 2001a, b; Underwood *et al.*, 2001a, b; Fenter *et al.*, 1995), as presented in Table 1. Here, the first group of  $\gamma_{\text{HNO}_3}$  has an order of magnitude from  $\sim 10^{-1}$  to  $\sim 10^{-2}$  (Umann *et al.*, 2005; Harnisch and Crowley, 2001a, b; Fenter *et al.*, 1995), compared to a range from  $\sim 10^{-3}$  to  $\sim 10^{-5}$  for the second group (Johnson *et al.*, 2005; Underwood *et al.*, 2001a, b).

The ultimate purpose of estimating (or measuring)  $\gamma_{\text{HNO}_3}$  is to apply the result to the chemistry-transport modeling studies. However, because of the large differences in the magnitude of  $\gamma_{\text{HNO}_3}$  onto dust particles, atmospheric modelers have been confused about which value should be adopted in their modeling studies (Song *et al.*, 2007; Bauer *et al.*, 2004; Zhang and Carmichael, 1999; Dentener *et al.*, 1996; and also the third group of  $\gamma_{\text{HNO}_3}$  as presented in Table 1). In addition, it appears that the parameterizations (or estimation method for  $\gamma_{\text{HNO}_3}$ ) for describing the heterogeneous interac-

**Table 1.** Reaction Probability of HNO<sub>3</sub> onto dust particles.

$\gamma_{\text{HNO}_3}$	Type of Dust	Method	Reference
$7.1 \times 10^{-2}$	Marble powder	Low pressure-flow reactor	Fenter <i>et al.</i> (1995)
$7.1 \times 10^{-2}$	CaCO <sub>3</sub>	(Knudsen cell)	
$7.6 \times 10^{-2}$	Na <sub>2</sub> CO <sub>3</sub>		
$1.5 (\pm 0.3) \times 10^{-1}$	CaCO <sub>3</sub> (humid)		
$6.0 \times 10^{-2}$	CaCO <sub>3</sub> (dried)		
$13.6 \times 10^{-2}$	Saharan Dust	Knudsen cell reactor	Harnisch and Crowley (2001a)
$17.1 (\pm 3) \times 10^{-2}$	Chinese Dust		
$14.0 (\pm 1.5) \times 10^{-2}$	Dolomite		
$11 (\pm 3) \times 10^{-2}$	Saharan Dust	Knudsen cell reactor	Harnisch and Crowley (2001b)
$6 (\pm 1.5) \times 10^{-2}$	Arizona Dust		
$10 (\pm 2.5) \times 10^{-2}$	CaCO <sub>3</sub> (heated)		
$18 (\pm 4.5) \times 10^{-2}$	CaCO <sub>3</sub> (unheated)		
$13 (\pm 3.3) \times 10^{-2}$	Al <sub>2</sub> O <sub>3</sub>		
$3.3 \times 10^{-2}$ <sup>1)</sup>	Saharan Dust	Field study	Umann <i>et al.</i> (2005)
$5.2 (\pm 0.3) \times 10^{-5}$	Gobi Dust	Knudsen cell reactor	Underwood <i>et al.</i> (2001a)
$2.0 (\pm 0.1) \times 10^{-5}$	Saharan Dust		
$1.4 \times 10^{-3}$	MgO (wet condition)	Knudsen cell reactor	Underwood <i>et al.</i> (2001b)
$1.6 \times 10^{-2}$	CaO (wet condition)		
$2 \times 10^{-5} \times R_G$ <sup>2)</sup>	Saharan Dust		
$1.1 \times 10^{-3}$	China Loess		
$7 (\pm 4) \times 10^{-4}$	Dolomite	Knudsen cell reactor	Johnson <i>et al.</i> (2005)
$1.5 (\pm 0.4) \times 10^{-3}$	CaCO <sub>3</sub>		
0.1	Dust	Modeling study	Dentener <i>et al.</i> (1996)
0.01	Dust	Modeling study	Zhang and Carmichael (1999)
0.1	Dust	Modeling study	Bauer <i>et al.</i> (2004)
$10^{-3}$ - $10^{-5}$ <sup>3)</sup>	Dust	—	This study

Note: <sup>1)</sup>Values of 0.017-0.054 were reported; <sup>2)</sup>Surface roughness factor; <sup>3)</sup>Values recommended by this study.

tion between HNO<sub>3</sub> and dust particles are questionable. Therefore, an impartial discussion is urgently required about both the magnitudes of  $\gamma_{\text{HNO}_3}$  onto dust particles and the parameterizations for the heterogeneous interactions between HNO<sub>3</sub> and dust particles. In this study, we discuss all the relevant and yet contentious issues regarding the heterogeneous processes between gas-phase HNO<sub>3</sub> and dust particles. In addition, through this study we wish to provide a modeler's perspective regarding the chemical evolution of dust particles and the magnitude of  $\gamma_{\text{HNO}_3}$  onto dust particles.

## 2. DISCUSSION

### 2.1 Research and Theoretical Background

The HNO<sub>3</sub> uptake into dust particles causes the replacement of carbonate (CO<sub>3</sub><sup>2-</sup>) originally associated with crustal Ca<sup>2+</sup> (and/or Mg<sup>2+</sup>) in dust particles via the following reaction:



Similar carbonate replacement reactions occur with the uptake of other acidic substances such as H<sub>2</sub>SO<sub>4</sub> and SO<sub>2</sub>. Based on this mechanism, Table 2 presents

the “dust chemical aging index”, defined as the ratio of estimated CO<sub>3</sub><sup>2-</sup> equivalence ([CO<sub>3</sub><sup>2-</sup>] in  $\mu\text{eq}/\text{m}^3$ ) to crustal cation equivalence ([Ca<sup>2+</sup>] + [Mg<sup>2+</sup>]) at several different locations in East Asia (Song *et al.*, 2007; 2005). As presented in Table 2, the ratios range from 0.39 to 0.87, indicating that the remaining carbonate fractions in the dust particles range from 39-87%, respectively, even after the chemical aging times of 24-84 hrs. Several single particle chemical analysis studies with East Asian dust particles reached the same conclusions (Ro *et al.*, 2005; Zhang *et al.*, 2003; Zhang and Iwasaka, 1999). The replaced CO<sub>3</sub><sup>2-</sup> fractions of 13-61% are believed to be released from dust particles by nitrate (and/or sulfate) formation. The small percentages of the replaced carbonate, even with the long chemical aging times, are obvious evidences of slow  $R_{\text{HNO}_3}$  onto dust particles.

Assuming pseudo first-order kinetics (eqn. 1),  $R_{\text{HNO}_3}$  can be calculated by eqns. (1) and (2). In the equations, the magnitude of  $R_{\text{HNO}_3}$  can be affected by three factors: i)  $\gamma_{\text{HNO}_3}$ ; ii) aerosol surface density ( $S_a$ ); and iii) gas-phase HNO<sub>3</sub> concentration ( $C_{\text{HNO}_3}$ ):

$$R_{\text{HNO}_3} = \frac{dC_{\text{HNO}_3}}{dt} = kC_{\text{HNO}_3} \quad (1)$$

**Table 2.** Average dust chemical aging indices and maximum HNO<sub>3</sub> uptake rates in East Asia.

Location	Date	$\frac{\overline{[CO_3^{2-}]}}{[Ca^{2+}]+[Mg^{2+}]}$ <sup>1)</sup>	$\overline{[NO_3^-]}^{\max}$ <sup>2)</sup> ( $\mu\text{g}/\text{m}^3$ )	$\frac{\Delta\overline{[NO_3^-]}^{\max}}{\Delta t}$ <sup>3)</sup> ( $\mu\text{g}/\text{m}^3 \cdot \text{hr}$ )	Chemical aging time <sup>4)</sup>
Yellow Sea					
ACE-ASIA C130 Flight #6	April 11, 2001	0.87	2.02	0.07	29 hours
ACE-ASIA C130 Flight #7	April 12, 2001	0.68	2.18	0.07	30 hours
Kyushu					
ACE-ASIA C130 Flight #8	April 13, 2001	0.39	1.89	0.05	42 hours
Seoul					
Case I	April 11, 2005	0.87	1.21	0.01	84 hours
Case II	April 15, 2005	0.43	5.65	0.23	25 hours
Case III	April 20, 2005	0.50	5.89	0.26	24 hours

<sup>1)</sup>Ratio averaged over the flight paths (ACE-ASIA Flights) and over the measured periods (Seoul).

<sup>2)</sup> $\overline{[NO_3^-]}^{\max} = \overline{[NO_3^-]} + \overline{[SO_4^{2-}]}$

<sup>3)</sup>The average production rate of  $\overline{[NO_3^-]}^{\max}$

<sup>4)</sup>Estimated elapsed times between pollution plume injections and measurements

$$k = \frac{1}{4} v_{HNO_3} \gamma_{HNO_3} S_a \quad (2)$$

where  $k$  denotes the mass transfer coefficient (1/s),  $v_{HNO_3}$  the molecular mean velocity of HNO<sub>3</sub> (cm/s), and  $S_a$  the aerosol surface density ( $\mu\text{m}^2/\text{cm}^3$ ). In this study, we discuss these three possibly influential factors to determine which factor (or factors) is really responsible for the observed discrepancy in  $R_{HNO_3}$  onto dust particles.

## 2.2 Reaction Probability of HNO<sub>3</sub> ( $\gamma_{HNO_3}$ )

First of all, the slow  $R_{HNO_3}$  could result from low  $\gamma_{HNO_3}$  onto dust particles. As mentioned in the Introduction, large differences have been reported in the magnitude of  $\gamma_{HNO_3}$  onto dust particles (Song *et al.*, 2007; Johnson *et al.*, 2005; Umann *et al.*, 2005; Harnisch and Crowley, 2001a,b; Underwood *et al.*, 2001a,b; Fenter *et al.*, 1995). Fig. 1 presents how fast HNO<sub>3</sub> can be transferred from the gas phase into dust particles with different  $\gamma_{HNO_3}$  values, using eqns. (1) and (2). For example, when  $\gamma_{HNO_3}=0.1$ , the 10 e-folding lifetime ( $\tau_{10}$ , defined as the time at which  $C_{HNO_3}/C_{HNO_3,0} = 1/10e = 0.037$ ;  $\tau_{10} = (1 + \ln 10)/k$ , where  $k$  represent the mass transfer coefficient in eqn. (2)) is only 1.41 hrs. When  $\gamma_{HNO_3}=0.01$ ,  $\tau_{10}$  becomes 8.03 hrs. In other words, 96.3% of HNO<sub>3</sub> is partitioned into the particulate phase within 8.03 hrs, when  $\gamma_{HNO_3}=0.01$ . The partitioned HNO<sub>3</sub> is then rapidly converted into nitrate, being associated with Ca<sup>2+</sup> and Mg<sup>2+</sup> ions inside the dust particles. For example, if the HNO<sub>3</sub> levels of 1-3 ppb are converted into nitrate at STP at a yield of 96.3%, nitrate concentrations of 2.6-7.7  $\mu\text{g}/\text{m}^3$  should be found in the dust particles after relatively short chemical aging times (within few hours). Once these amounts of nitrate are formed in the dust particles, the particles

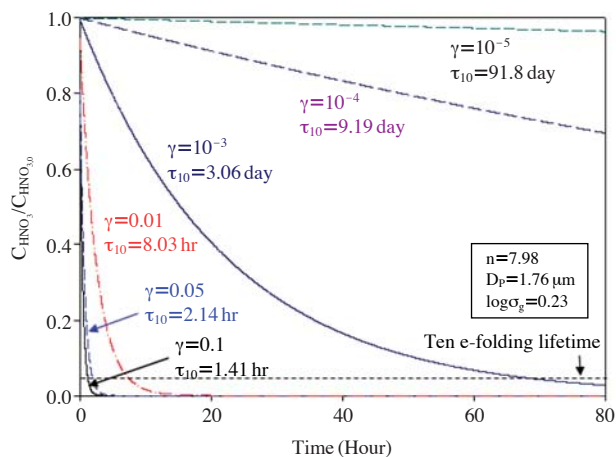


**Fig. 1.** Ten e-folding lifetimes ( $\tau_{10}$ ) with different reaction probability of HNO<sub>3</sub>. The parameters for log-normal aerosol distribution used in this figure are presented in the box (Zhang *et al.*, 1994).

(particularly Ca<sup>2+</sup>) can be completely neutralized only by nitrate in most typical dusty situations. HNO<sub>3</sub> levels of 1-3 ppb were frequently observed with high dust concentrations over the downwind areas from the polluted regions in East Asia (this will be discussed in more detail in section 2.4; also refer to Bauer *et al.* (2004)). However, such large amounts of nitrate have never been found in dust particles, particularly in East Asia (Song *et al.*, 2007; Ro *et al.*, 2005; Song *et al.*, 2005; Zhang *et al.*, 2003). In contrast, when  $\gamma_{HNO_3} = 10^{-3}$ - $10^{-5}$ ,  $R_{HNO_3}$  become much slower ( $\tau_{10}=3.1$ -91.8 days). With the initial  $C_{HNO_3}$  of 1-3 ppb and  $\gamma_{HNO_3}$  of  $10^{-4}$ , the converted amount of nitrate after the interacting times of 8 hours is 0.095-0.29  $\mu\text{g}/\text{m}^3$ , which is

equivalent to an hourly averaged  $R_{HNO_3}$  of 0.01-0.04  $\mu\text{g}/\text{m}^3 \cdot \text{hr}$ . Such slow  $R_{HNO_3}$  are more consistent with the slow chemical evolution of dust particles observed in the field measurements. For example, in Table 2, we estimated the possibly maximum nitrate concentrations ( $[\text{NO}_3^-]_{\text{max}}$ ;  $[\text{NO}_3^-]_{\text{max}} = [\text{NO}_3^-] + [\text{SO}_4^{2-}]$ ). The measurement data used in Table 2 were obtained from the ACE-ASIA C130 flight campaign conducted over the Yellow sea on April 11-13, 2001, and a measurement campaign conducted in Seoul in April, 2005. We selected the data from the dust storm periods of the campaigns. In this calculation, while we cannot estimate the individual amounts of nitrate and sulfate, we can estimate the combined amounts of “nitrate+sulfate” concentration in the dust particles by equating the replaced carbonate equivalences to the “nitrate+sulfate” equivalences. In an extreme case, carbonate in dust particles could be replaced only by  $\text{NO}_3^-$ . These amounts ( $[\text{NO}_3^-]_{\text{max}} = [\text{NO}_3^-] + [\text{SO}_4^{2-}]$ ) are then divided by chemical aging times to obtain the maximum possible nitrate uptake rates. As shown in Table 2, the rates range from 0.01 to 0.26  $\mu\text{g}/\text{m}^3 \cdot \text{hr}$ . These values are in general comparable to the estimated rates above (0.01-0.04  $\mu\text{g}/\text{m}^3 \cdot \text{hr}$ ), particularly for the cases of ACE-ASIA C-130 Flights #6, #7, and #8 which recorded results in the range 0.05-0.07  $\mu\text{g}/\text{m}^3 \cdot \text{hr}$  (again, it is important to remember that the average uptake rates actually represent the production rates of  $\text{NO}_3^- + \text{SO}_4^{2-}$ ).

Although in this study we do not intend to estimate  $\gamma_{HNO_3}$  onto dust particles, one of the objectives of this study is to decide which values of “already-measured”  $\gamma_{HNO_3}$  in Table 1 can be adopted in the dust chemistry modeling studies. Based on the calculations above, the modeling studies with  $\gamma_{HNO_3}$  of  $\sim 10^{-3}$ – $\sim 10^{-5}$  could produce more consistent results with the field measurement data.

### 2.3 Surface Area

There is another possible mechanism that could slow down  $R_{HNO_3}$  into dust particles: the application of a

smaller surface area to eqn. (2). For example, in an estimating procedure of  $\gamma_{HNO_3}$ , Umann *et al.* (2005) introduced an “active surface area ( $S_A$ )” (for greater detail, refer to both Umann *et al.* (2005) and Matter Engineering, Appendix IV of Operating Instructions LQ1-DC, SKM990318-7b). A similar type of active surface area, so-called “Fuchs surface”, was also introduced by Pandis *et al.* (1991) and Shi *et al.* (2001). Whichever active surface area is used,  $S_A$  has a tendency to become smaller than the “geometric surface area” ( $S_G$ ), when the coarse-mode fraction is large, such as in dust and sea-salt aerosol cases. Therefore, if we use  $S_A$  instead of  $S_G$  for the gas-to-particle mass transfer process,  $R_{HNO_3}$  could become slow. Table 3 presents the typical ratios of  $S_A$  to  $S_G$  for dust and sea-salt particle distributions (Sander and Crutzen, 1996; Zhang *et al.*, 1994; Jaenicke, 1993). The ratios range between 0.11 and 0.41. In particular the ratio is 0.11 for the two typical dust cases, indicating that  $R_{HNO_3}$  become slower by a factor of 0.11, even if the same  $\gamma_{HNO_3}$  is used. Here, the relevant question is whether  $S_A$  can be applied to eqn. (2). Umann *et al.* (2005) used  $S_A$  with the concept of the “actual surface area” that is accessible for impinging gas molecules that can typically be measured by a BET (Brunauer, Emmett and Teller) type of instrument. However, both the active ( $\mu\text{m}^2/\text{cm}^3$ ) and Fuchs ( $1/\text{cm}^3$ ) surface areas are not the “actual/accessible surface area”, but an imaginary aerosol-surface area conveniently adjusted to consider the changing mechanism in the gas-to-particle mass transfer in accordance with the aerosol size changes (Pandis *et al.*, 1991). For the fine particles, the gas-to-particle mass transfer (uptake) rates are proportional to the second moment (i.e., surface area), whereas for the coarse particles,  $R_{HNO_3}$  are proportional to the first moment (i.e., radius). Therefore, the  $S_A$ -to- $S_G$  ratios are small when the coarse aerosol fraction is large, whereas the ratios are close to unity when the fine fraction is dominant. The variation in uptake mechanism with the aerosol size can be taken into account by the use of Fuchs and Sutugin kinetics (1971) or other

**Table 3.** Mass transfer coefficients with different types of surface area ( $\gamma_{HNO_3}=0.033$ ).

Aerosol type and size distribution	$S_G$ ( $\mu\text{m}^2/\text{cm}^3$ )	$S_A$ ( $\mu\text{m}^2/\text{cm}^3$ )	$S_A/S_G$	$k_A$ (1/s)	$k_G$ (1/s)	$k_F$ (1/s)
Dust						
Jaenicke (1993) <sup>1)</sup>	149.48	16.65	0.11	$4.26 \times 10^{-5}$	$3.82 \times 10^{-4}$	$2.63 \times 10^{-4}$
Zhang <i>et al.</i> (1994) <sup>2)</sup>	137.07	15.72	0.11	$4.02 \times 10^{-5}$	$3.50 \times 10^{-4}$	$3.12 \times 10^{-4}$
Sea salt						
Jaenicke (1993)	44.54	18.06	0.41	$4.97 \times 10^{-5}$	$1.36 \times 10^{-4}$	$1.15 \times 10^{-4}$
Sander and Crutzen (1996) <sup>3)</sup>	71.08	5.15	0.07	$1.32 \times 10^{-5}$	$1.82 \times 10^{-4}$	$1.45 \times 10^{-4}$

<sup>1)</sup> The parameters have also appeared in Seinfeld and Pandis (1998) (see p. 430)

<sup>2)</sup>  $n=7.98$ ;  $r_p=0.88 \mu\text{m}$ ;  $\log\sigma_g=0.23$

<sup>3)</sup>  $n=1.40$ ,  $r_p=1.66 \mu\text{m}$ ;  $\log\sigma_g=0.19$

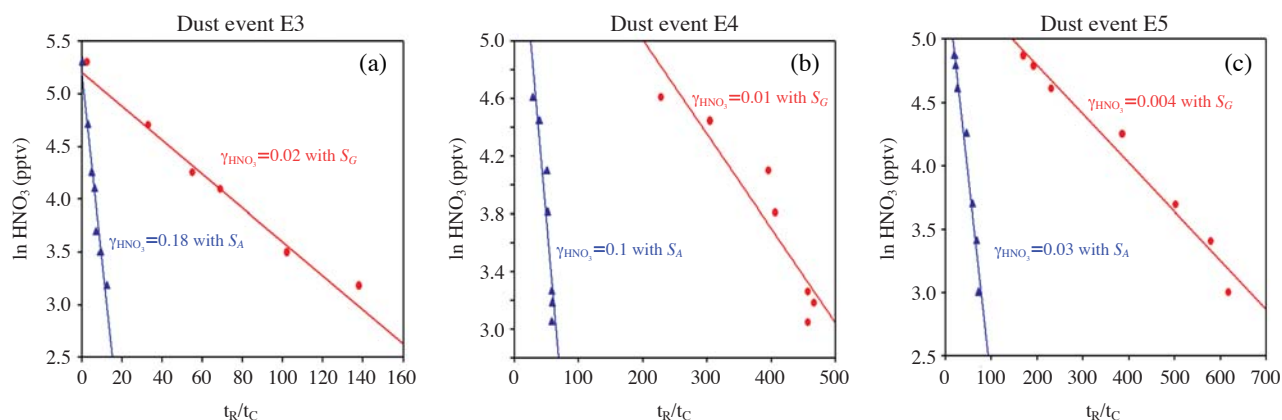


Fig. 2. Estimation of  $\gamma_{\text{HNO}_3}$  with two different types of surface areas ( $S_A$  and  $S_G$ ).

similar kinetics (e.g., see p. 604 in Seinfeld and Pandis, 1998). In Table 3, the Fuchs-Sutugin mass transfer coefficient ( $k_F$ ) is compared with  $k_A$  ( $k$  from eqn. 2 with  $S_A$  for  $S_a$ ) and  $k_G$  ( $k$  from eqn. 2 with  $S_G$  for  $S_a$ ). As shown in Table 3, the values of  $k_G$  are consistent with  $k_F$ , whereas the values of  $k_A$  are smaller than  $k_F$  by a factor of  $\sim 0.1$ . Meanwhile, the use of  $S_A$  in eqn. (2) also leads to an erroneous estimation of  $\gamma_{\text{HNO}_3}$ . One example of the erroneous results is shown in Fig. 2. Umann *et al.* (2005) estimated  $\gamma_{\text{HNO}_3}$  from the field measurements in Sahara desert, using equations (1) and (2) with  $S_A$ . We selected three dust episodes (E3, E4, and E5) from Umann *et al.*'s work (2005), and then re-estimated  $\gamma_{\text{HNO}_3}$  with  $S_A$  and  $S_G$ . As shown in Fig. 2, when  $S_G$  is used instead of  $S_A$ , the values of  $\gamma_{\text{HNO}_3}$  are decreased down to 0.004–0.02, which are smaller than Umann *et al.*'s values ( $\gamma_{\text{HNO}_3}=0.03$ –0.18). These values are also closer to the second group of  $\gamma_{\text{HNO}_3}$  in Table 1 that we recommended to be used in the future dust chemistry modeling studies.

## 2.4 HNO<sub>3</sub> Concentration in the Gas Phase ( $C_{\text{HNO}_3}$ )

The third factor that could affect  $R_{\text{HNO}_3}$  into dust particles is  $C_{\text{HNO}_3}$  (from eqn. 1). If  $C_{\text{HNO}_3}$  is low,  $R_{\text{HNO}_3}$  becomes slow. Or, if the amounts of HNO<sub>3</sub> are not sufficient, the amounts of nitrate formed in dust particles can be limited by the insufficient the amounts of HNO<sub>3</sub>, even with fast  $R_{\text{HNO}_3}$ . Particularly, extremely low  $C_{\text{HNO}_3}$  could occur over the areas where NH<sub>3</sub> concentrations are high. Over such areas, HNO<sub>3</sub> can be depleted by the reaction of  $\text{HNO}_3(\text{g}) + \text{NH}_3(\text{g}) \rightarrow \text{NH}_4\text{NO}_3(\text{aerosol})$ . For example, East Asia has large NH<sub>3</sub> emissions (Kim *et al.*, 2006). Fig. 3 presents  $C_{\text{HNO}_3}$  and the Ca<sup>2+</sup> concentrations measured by TRACE-P DC-8 Flights #9 and #13 over the Yellow Sea and East China Sea (see panels (c) and (g)). As presented in pan-

els (d) and (h), the air masses originated from the Gobi desert and the arid areas in Inner Mongolia, and then passed through the highly polluted, high NO<sub>x</sub> and NH<sub>3</sub> emission areas in China such as Beijing, Tianjin, Qingdao, Dalian, Nanjing, and Shanghai, as well as various Chinese agricultural areas (Kim *et al.*, 2006). The high levels of Ca<sup>2+</sup> indicate that the air masses intercepted by DC-8 Flights #9 and #13 contained high levels of dust particles. In the two flights, the observed levels of HNO<sub>3</sub> were increased up to as high as 7 ppb (see panel (g)). The typical HNO<sub>3</sub> levels reported from other TRACE-P DC-8 and P3-B flights in the boundary layer under the continental outflow situations ranged between  $\sim 1$  ppb and  $\sim 3$  ppb. Despite the coexistence of the high levels of dust particles and HNO<sub>3</sub>, Song *et al.* (2007; 2005) reported very low nitrate (and/or sulfate) concentrations inside dust particles over the areas close to the flight paths of TRACE-P DC-8 Flights #9 and #13. This is an important correction to the results from Meskhidze *et al.* (2003). They insisted that the coexistence of high levels of Ca<sup>2+</sup> and HNO<sub>3</sub> in the TRACE-P DC-8 Flight #13 was firm evidence that HNO<sub>3</sub> had already filled up the dust particles (i.e., complete neutralization of Ca<sup>2+</sup> or 100% carbonate replacement had occurred).

Again, the presence of high HNO<sub>3</sub> levels indicates that the low nitrate concentrations in the dust particles were not a result of the low  $C_{\text{HNO}_3}$  levels, but were rather due to the small  $\gamma_{\text{HNO}_3}$  that was reduced even smaller than  $10^{-3}$ .

## 3. CONCLUSIONS

The observed  $R_{\text{HNO}_3}$  onto dust particles were much slower than previously estimated. In addition,  $R_{\text{HNO}_3}$  have been overestimated in several previous dust

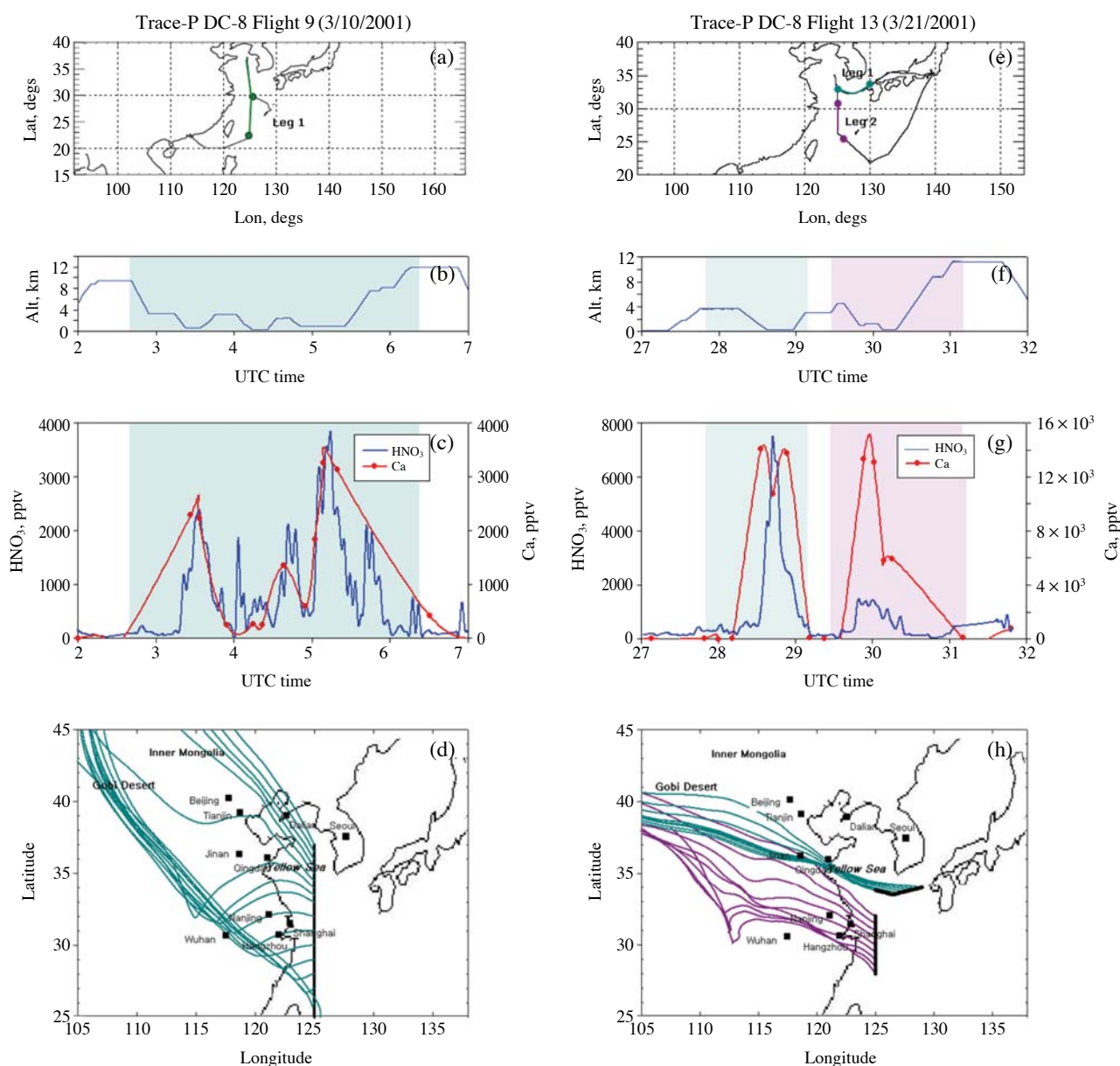


**Fig. 3.** The  $\text{HNO}_3$  and  $\text{Ca}^{2+}$  concentrations encountered by TRACE-P DC-8 Flights #9 and #13: (a) and (e) flight paths; (b) and (f) altitudes of the flights; (c) and (g)  $\text{HNO}_3$  and  $\text{Ca}^{2+}$  concentrations; and (d) and (h) five-day backward trajectory analyses, respectively, using the HYSPLIT model and meteorological data available on the NOAA/ARL web site (Draxler and Hess, 1998).

modeling studies, for which three possibilities were discussed here: (1) the magnitude of  $\gamma_{\text{HNO}_3}$ , (2) aerosol surface area, and (3)  $C_{\text{HNO}_3}$ . Regarding the second factor, we suggested that  $S_G$  should be used in eqn. (2) instead of  $S_A$ , which had been used, for example, in Umann *et al.*'s study (2005). With respect to the third factor, we showed that the observed  $C_{\text{HNO}_3}$  was relatively high, sometimes increasing up to as high as  $\sim 7$  ppb in the marine boundary layer in East Asia, for example.  $C_{\text{HNO}_3}$  can not limit nitrate formation in dust particles.

The over-predicted  $R_{\text{HNO}_3}$  onto the dust particles may have been caused by the first factor-overestimated  $\gamma_{\text{HNO}_3}$  values ( $\gamma_{\text{HNO}_3} = 10^{-1}$ - $10^{-2}$ ). In the previous modeling studies of Dentener *et al.* (1996), Zhang and Carmichael (1999), and Bauer *et al.* (2004),  $\gamma_{\text{HNO}_3}$  values of 0.1 and 0.01 were used. In contrast to these overestimated  $\gamma_{\text{HNO}_3}$  values, smaller  $\gamma_{\text{HNO}_3}$  values within the range  $10^{-3}$ - $10^{-5}$  have also been reported by Underwood *et al.* (2001a, b) and Johnson *et al.* (2005). In this study we concluded that the use of  $\gamma_{\text{HNO}_3}$  values between

$\sim 10^{-3}$  and  $\sim 10^{-5}$  could produce more realistic results than those within the range of  $10^{-1}$ - $10^{-2}$  could, by more accurately predicting the nitrate formation characteristics in dust particles.

## ACKNOWLEDGEMENTS

This work was financially supported by the Mid-Career Research Program, through a National Research Foundation of Korea (NRF) grant from the Ministry of Education, Science and Technology (MEST) (2010-0014058); and a National Research Foundation of Korea (NRF) grant funded by the Korea government (MEST) (No. R17-2008-042-01001-0).

## REFERENCES

- Bauer, S.E., Balkanski, Y., Schulz, M., Hauglusteine, D. (2004) Global modeling of heterogeneous chemistry on mineral aerosol surfaces: Influence on tropospheric ozone chemistry and comparison to observations. *Journal of Geophysical Research-Atmospheres* 109, D02304, doi:10.1029/2003JD003868.
- Dentener, F.J., Carmichael, G.R., Zhang, Y., Lelieveld, J., Crutzen, P.J. (1996) Role of mineral aerosol as a reactive surface in the global troposphere. *Journal of Geophysical Research-Atmospheres* 101, 22869-22889.
- Draxler, R.R., Hess, G.D. (1998) An overview of the HYSPLIT\_4 modeling system for trajectories, dispersion and deposition. *Australian Meteorological Magazine* 47(4), 295-308.
- Fenter, F., Caloz, F., Rossi, M.J. (1995) Experimental evidence for the efficient "Dry deposition" of nitric acid on calcite. *Atmospheric Environment* 29(22), 3365-3327.
- Fuchs, N.A., Sutugin, A.G. (1971) High dispersed aerosols, in *Tropics in Current Aerosol Research* (Hidy, G.M. and Brock, J.R. Eds), Peragamon, New York, pp. 1-200.
- Hanisch, F., Crowley, J.N. (2001a) Heterogeneous reactivity of gaseous nitric on authentic mineral dust samples, and on individual mineral and clay mineral components. *Physical Chemistry Chemical Physics* 3, 2474-2482.
- Hanisch, F., Crowley, J.N. (2001b) Heterogeneous reactivity of gaseous nitric acid on Al<sub>2</sub>O<sub>3</sub>, CaCO<sub>3</sub>, and atmospheric dust samples: A Knudsen cell study. *Journal of Physical Chemistry A* 105, 3096-3106.
- Jaenicke, R. (1993) Troposphere aerosols, in *Aerosol-Cloud-Climate Interactions* (Hobbs, P.V. Ed.), Academic Press, San Diego, pp. 1-31.
- Johnson, E.R., Sciegienka, J., Carlos-Cuellar, S., Grassian, V.H. (2005) Heterogeneous uptake of gaseous nitric acid on dolomite (CaMg(CO<sub>3</sub>)<sub>2</sub>) and calcite (CaCO<sub>3</sub>) particles: A Knudsen cell study using multiple, single, and fractional particle layers. *Journal of Physical Chemistry A* 109, 6901-6911.
- Kim, K.J., Song, C.H., Ghim, Y.S., Won, J.G., Yoon, S.C., Carmichael, G.R., Woo, J.-H. (2006) An investigation on NH<sub>3</sub> emissions and particulate NH<sub>4</sub><sup>+</sup> and NO<sub>3</sub><sup>-</sup> formation in East Asia. *Atmospheric Environment* 40, 2139-2150.
- Maxwell-Meier, K., Weber, R.J., Song, C.H., Orsini, D., Ma, Y., Carmichael, G.R., Streets, D.G., Blomquist, B. (2004) Inorganic composition of fine particles in mixed mineral dust-pollution plumes observed from airborne measurements during ACE-Asia. *Journal of Geophysical Research-Atmospheres* 109, D19S07, doi:10.1029/2003JD004464.
- Meskhidze, N., Chameides, W.L., Nenes, A., Chen, G. (2003) Iron mobilization in mineral dust: Can anthropogenic SO<sub>2</sub> emissions affect ocean productivity. *Geophysical Research Letters* 30(21), 2085, doi:10.1029/2003GL018035.
- Pandis, S.N., Baltensperger, U., Wolfenbarger, J.K., Seinfeld, J.H. (1991) Inversion of aerosol data from the epiphonometer. *Journal of Aerosol Science* 22(4), 417-428.
- Ro, C.-U., Hwang, H., Kim, H., Chun, Y., Van Grieken, R. (2005) Single particle characterization of four "Asian Dust" samples collected in Korea, using low-Z particle electron probe X-ray microanalysis. *Environmental Science & Technology* 39, 1409-1419.
- Sander, R., Crutzen, P.J. (1996) Model study indicating halogen activation and ozone destruction in polluted air masses transported to the sea. *Journal of Geophysical Research-Atmospheres* 101, D4, doi:10.1029/95JD03793.
- Seinfeld, J.H., Pandis, S.N. (1998) *Atmospheric chemistry and physics*. A Wiley-Interscience Publication, New York, p. 604.
- Shi, J.P., Harrison, R.M., Evans, D. (2001) Comparison of ambient particle surface area measurement by epiphaniometer and SMPS/APS. *Atmospheric Environment* 35, 6193-6200.
- Song, C.H., Carmichael, G.R. (2001) Gas-particle partitioning of nitric acid modulated by alkaline aerosol. *Journal of Atmospheric Chemistry* 40, 1-22.
- Song, C.H., Maxwell-Meier, K., Weber, R.J., Kapustin, V., Clarke, A. (2005) Dust composition and mixing state inferred from airborne composition measurements during ACE-Asia C130 Flight#6. *Atmospheric Environment* 39, 359-369.
- Song, C.H., Kim, C.M., Lee, Y.J., Carmichael, G.R., Lee, B.K., Lee, D.S. (2007) An evaluation of reaction probabilities of sulfate and nitrate precursors onto East Asian dust particles. *Journal of Geophysical Research-Atmospheres* 112, D18206, doi:10.1029/2006JD008092.
- Umann, B., Arnold, F., Schaal, C., Hanke, M., Uecker, J., Aufmhoff, H., Balkanski, Y., Van Dingenen, R. (2005) Interaction of mineral dust with gas phase nitric acid and sulfur dioxide during the MINATORIC II field

- campaign: First estimate of the uptake coefficient  $\gamma_{\text{HNO}_3}$  from atmospheric data. *Journal of Geophysical Research-Atmospheres* 110, 22306-22323.
- Underwood, G.M., Li, P., Al-Abadleh, H., Grassian, V.H. (2001a) A knudsen cell study of the heterogeneous reactivity of nitric acid on oxide and mineral dust particles. *Journal of Physical Chemistry A* 105, 6609-6620.
- Underwood, G.M., Song, C.H., Phadnis, M., Carmichael, G.R., Grassian, V.H. (2001b) Heterogeneous reactions of  $\text{NO}_2$  and  $\text{HNO}_3$  on oxides and mineral dust: A combined laboratory and modeling study. *Journal of Geophysical Research-Atmospheres* 106, 18055-18066.
- Zhang, D., Iwasaka, Y. (1999) Nitrate and sulfate in individual Asian dust-storm particles in Beijing, China in the spring of 1995 and 1996. *Atmospheric Environment* 33, 3213-3223.
- Zhang, D., Zang, J., Shi, G., Iwasaka, Y., Matsuki, A., Trochkin, D. (2003) Mixture of individual Asian dust particles at a coastal site of Qingdao, China. *Atmospheric Environment* 37, 3895-3901.
- Zhang, Y., Sunwoo, Y., Kothamarthi, V., Carmichael, G.R. (1994) Photochemical oxidant processes in the presence of dust: An evaluation of the impact of dust on particulate nitrate and ozone formation. *Journal of Applied Meteorology* 33, 813-824.
- Zhang, Y., Carmichael, G.R. (1999) The role of mineral aerosol in tropospheric chemistry in East Asia-A model study. *Journal of Applied Meteorology* 38(3), 353-366.

(Received 4 April 2011, accepted 22 April 2011)